R. & M. No. 3543

MINISTRY OF TECHNOLOGY

AERONAUTICAL RESEARCH COUNCIL
REPORTS AND MEMORANDA

Minimum Drag Surfaces of given Lift which Support Two-Dimensional Supersonic Flow Fields

By J. PIKE

LONDON: HER MAJESTY'S STATIONERY OFFICE
1968
PRICE 12*s.* 6*d.* NET

Minimum Drag Surfaces of given Lift which Support Two-Dimensional Supersonic Flow Fields

By J. Pike

Reports and Memoranda No. 3543*
September, 1966

Summary.

The two-dimensional surface giving minimum pressure drag for given lift coefficient in supersonic flow is considered. The method adopted is a small perturbation of a plane surface; the pressure is expressed as a power series in the perturbed slope and third order terms are neglected. The shape of the optimum surface is found to be a double wedge surface, with a single discontinuity in the surface slope. The compression surface is concave at the discontinuity for Mach numbers below about 1·4 and above 3, and between these it can be slightly convex.

The performance in the case $\gamma = 1{\cdot}4$ is compared with that of the plane wedge, and the improvement is found to be very small, except at hypersonic speeds when improvements greater than 1 per cent are obtained.

Similar results hold for waveriders (three-dimensional wing shapes) based on two-dimensional flow fields.

CONTENTS

1. *Introduction.*

It is well known that within the limitations of small disturbance theory (applicable to low supersonic Mach numbers), the optimum lifting two-dimensional surface is a flat plate[1]. At high supersonic and

*Replaces R.A.E. Tech. Report No. 66 305—A.R.C. 28 825.

hypersonic Mach numbers we can no longer justify *a priori* the use of small disturbance theory, except for very small flow deflection. To find the optimum surface at these Mach numbers a more accurate description of the flow is required. The method adopted in the present paper is to take the exact solution for the flow about a plane wedge given by the oblique shock wave relationships[2] and to consider the direct effect of deviations from the plane wedge shape by means of Busemann second-order theory, while the effect of reflections from the shock wave is treated linearly. Reflected disturbances from the shock wave are generally much smaller than the incident disturbances. The optimum two-dimensional surfaces are found to be 'double wedge' surfaces, concave above $M_\infty = 3$. The optimum three-dimensional waveriders based on two-dimensional flow fields also are concave chordwise above $M_\infty = 3$.

Recently the case of small incidence at very high Mach numbers has been treated by Cole and Aroesty[3] using hypersonic small disturbance theory. They find that the improvement in drag relative to that of plane wedge is proportional to the size of perturbation from the wedge, and suggest that the optimum shape within their constraints is a 'multi-wedge'. Here it is shown that the strict optimum approximates closely to a double wedge and the maximum improvement in performance is about 1 per cent in air.

In this Report wedges and waveriders are compared which have the same lift coefficient. An alternative approach is to compare shapes with the same volume. The method used in this Report is not applicable to the constant volume constraint. However, Bartlett[4] has investigated a series of shapes with double wedge lower surfaces and streamwise upper surfaces, which have constant volume. Using shock expansion theory, he finds that the double wedges with the maximum lift-drag ratio are markedly convex, and have lift-drag ratios of up to 4 per cent greater than the plane wedge with a streamwise upper surface. It should be noted that the difference in the results is due solely to the different constraints.

2. *The Pressure on a Nearly Plane Two-Dimensional Surface.*

Consider a plane surface inclined at an angle δ_0 to the free stream (e.g. Fig. 1). Neglecting viscous effects the shock wave is plane, and flow conditions behind the shock wave are constant. A small perturbation $\delta(x)$ in the surface slope causes a small change in pressure. The change in pressure at any point x_1 on the surface due to δ at that point can be estimated by Busemann second order theory based on the flow conditions behind the shock wave,

i.e.

$$\frac{p-p_0}{q_0} = C_1\,\delta(x_1)+C_2\,\delta^2(x_1) \tag{1}$$

where

$$C_1 = \frac{2}{(M_0^2-1)^{\frac{1}{2}}}, \quad C_2 = \frac{(\gamma+1)\,M_0^4-4(M_0^2-1)}{2(M_0^2-1)^2}$$

and p_0, q_0, M_0 are respectively the static pressure, dynamic pressure and Mach number behind the shock wave. The values of C_1 and C_2 are shown in Fig. 2.

For a plane surface the characteristic lines of the flow are straight and inclined at the Mach angle to the flow direction (Fig. 3). A small disturbance created at A propagates along the characteristic AB and is reflected from the shock wave at B. The reflected disturbance (its strength attenuated by a factor λ) propagates along BC and is reflected at C without attenuation, doubling the effect of the reflected disturbance on the surface. The ratio OA/OC (denoted by k) is independent of the position of A for a plane surface; that is

$$k = \frac{OA}{OC} = \frac{OD-AD}{OD+DC} = \frac{1-\beta\tan(\theta-\delta_0)}{1+\beta\tan(\theta-\delta_0)} \tag{2}$$

where

$$\beta = \cot \mu = (M_0^2 - 1)^{\frac{1}{2}} \qquad (\textit{see } \text{Fig. 4}).$$

For the perturbed surface k is constant to first order. Using a linearised estimate of the pressure change due to δ (i.e. $(p-p_1)/q_1 = C_1 . \delta$), Chernyi[5] finds that the pressure change at any point on the surface (x_1) due to $\delta(x)$ is (including reflected pressure changes),

$$\frac{p-p_0}{q_0} = C_1 \left(\delta(x_1) + 2 \sum_{n=1}^{\infty} \lambda^n \, \delta(k^n x_1) \right). \tag{3}$$

The term in equation (3) containing λ represents the pressure change due to reflections from the shock wave. The value of the reflection coefficient, λ, (i.e. the attenuation of a disturbance on reflection from the shock wave) is shown in Fig. 5 for $\gamma = 1{\cdot}4$, reproduced from Ref. 5. Over a large range of values of δ_0 and free stream Mach number the value of λ is small. The term in λ (of order $\lambda\delta$), is then of second order, and the change in pressure or M_0 at the surface point x_1 due to reflections is therefore also of second order. The appropriate second order expression for the direct effect of $\delta(x)$ on the pressure is equation (1), and this replaces the term $C_1 \, \delta(x_1)$ in equation (3) to give the complete second order expression (with the suffix on x_1 discarded):

$$\frac{p-p_0}{p_0} = C_1 \, \delta(x) + C_2 \, \delta^2(x) + 2\lambda \, C_1 \, \delta(kx). \tag{4}$$

A refinement of this expression (still accurate only to second order) is obtained by assuming $\delta(k^n x) = \delta(kx)$, instead of the assumption used to obtain equation (4) (i.e. $\delta(k^n x) = 0$ for $n \geqq 2$). As

$$\lambda + \lambda^2 + \lambda^3 + \lambda^4 \ldots . = \lambda/(1-\lambda)$$

the term in λ of equation (3) can be assumed to give $2\lambda \, \delta(kx)/(1-\lambda)$ and the equation equivalent to equation (4) is

$$\frac{p-p_0}{q_0} = C_1 \, \delta(x) + C_2 \, \delta^2(x) + \frac{2\lambda \, C_1 \, \delta(kx)}{1-\lambda}. \tag{5}$$

The advantage of this refinement becomes apparent later, for although it does not affect the assumptions for which the optimum surface is obtained (i.e. second order accuracy), it is found to be a more accurate approximation for evaluating the performance of the surfaces.

3. *The Lift and Drag of a Nearly Plane Two-Dimensional Surface.*

The lift per unit span of the two-dimensional surface of unit chord is given by

$$L = \int_0^1 (p - p_r) \, dx \tag{6}$$

where p_r is a reference pressure. Hence substituting for p from equation (5),

$$L = \int_0^1 (p_0 - p_r) \, dx + q_0 \int_0^1 \left(C_1 \, \delta(x) + C_2 \, \delta^2(x) + \frac{2\lambda C_1}{1-\lambda} \, \delta(kx) \right) dx. \tag{7}$$

If $\delta(x)$ produces no change in lift

$$\int_0^1 \left(\delta(x)+\frac{C_2}{C_1}\delta^2(x)+\frac{2\lambda}{1-\lambda}\delta(kx)\right)dx = 0\,. \tag{8}$$

Let

$$F(x) = \delta(x) \quad \text{for} \quad 0 \leqq x \leqq k \tag{9}$$

$$H(x) = \delta(x) \quad \text{for} \quad k \leqq x \leqq 1\,. \tag{10}$$

Then F and H are independent functions, for they define x over different intervals.
Let

$$F_n = \int_0^1 F^n\,dx \quad \text{and} \quad H_n = \int_k^1 H^n\,dx\,. \tag{11}$$

Equation (8) can then be written

$$F_1+H_1+\frac{C_2}{C_1}(F_2+H_2)+\frac{2\lambda}{(1-\lambda)k}F_1 = 0\,. \tag{12}$$

The drag per unit span of the two-dimensional surface is given by

$$D = \int_0^1 (p-p_r)\tan(\delta_0+\delta)\,dx\,. \tag{13}$$

Expanding $\tan(\delta_0+\delta)$ in a Taylor series this becomes

$$D = \tan\delta_0\int_0^1 (p-p_r)\,dx+\sec^2\delta_0\int_0^1 (p-p_r)\,\delta dx$$

$$+\sec^2\delta_0\tan\delta_0\int_0^1 (p-p_r)\,\delta^2\,dx+0(\delta^3) \tag{14}$$

Substituting for p from equation (5)

$$\frac{D-D_0}{\sec^2\delta_0} = \int_0^1 (p_0-p_r)\,\delta dx+\tan\delta_0\int_0^1 (p_0-p_r)\,\delta^2\,dx+q_0\int_0^1 C_1\,\delta^2\,dx+0(\delta^3,\lambda\delta^2) \tag{15}$$

which becomes, using equations (11)

$$\frac{D-D_0}{\sec^2\delta_0} = (p_0-p_r)(F_1+H_1)+\{(p_0-p_r)\tan\delta_0+q_0\,C_1\}(F_2+H_2)+0(\delta^3,\lambda\delta^2) \tag{16}$$

Substituting for F_1+H_1 from equation (12)

$$\frac{D-D_0}{(p_0-p_r)\sec^2\delta_0} = -\frac{2\lambda}{1-\lambda}\cdot\frac{F_1}{k}+\left\{\tan\delta_0+\frac{q_0\,C_1}{p_0-p_r}-\frac{C_2}{C_1}\right\}(F_2+H_2)\,. \tag{17}$$

4. *The Minimum Drag Surface.*

In Section 3 an expression for the drag (equation (17)) and a constant lift condition (equation (12)), are derived in terms of two arbitrary functions F and H, describing the surface slope over particular regions of the surface. The optimum surface is given by the F and H which minimise the drag under the constant lift constraint. The process adopted to find this F and H takes place in several steps. First it is shown that for any given $F(x)$, the function H which minimises the drag is a constant. This must also be the form of H for the unrestricted minimum drag surface, for if H were not constant for this surface, then whatever $F(x)$, the drag could be reduced by using constant H. With H constant, optimising for F shows F to be constant also. The optimum surface is thus shown to be a double wedge, with wedge angles δ_0+F and δ_0+H to the free stream (e.g. Fig. 6). The two constants F and H are related by the constant lift condition. Hence the drag can be represented as a function of F only, and as a final step, the minimum drag is found by putting $dD/dF = 0$.

For any function F the values of F_1 and F_2 are constant. Then the drag, from equation (17) can be written

$$\frac{D-D_0}{(p_0-p_r)\sec^2\delta_0} = \left\{\tan\delta_0+\frac{q_0\,C_1}{p_0-p_r}-\frac{C_2}{C_1}\right\}\int_k^1 H^2\,dx+\text{constant} \tag{18}$$

and the constant lift condition becomes

$$C_1\int_k^1 H\,dx+C_2\int_k^1 H^2\,dx = \text{constant}\,. \tag{19}$$

The coefficient of H_2 in the drag expression can be negative if the lower surface Mach number is sufficiently close to 1, but in the cases of interest it is always positive, so that the minimum drag is given by minimum H_2, under the constraint of equation (19). This is a straightforward problem in the calculus of variations. In the usual way, we define a function P by

$$P = H^2+\mu(C_1\,H+C_2\,H^2) \tag{20}$$

where μ is a Lagrange multiplier. Then H is the required optimum function if it satisfies $dP/dH = 0$; i.e.

$$2H+C_1\,\mu+2\mu\,C_2\,H = 0\,. \tag{21}$$

Hence the optimum H is a constant, a result which can be confirmed intuitively from the original problem.

With H constant, $H_1 = (1-k)\,H$ and $H_2 = (1-k)\,H^2$. The drag expression and lift condition can now be written in terms of F_1 and F_2.

i.e.

$$\frac{D-D_0}{(p_0-p_r)\sec^2\delta_0} = \frac{-2\lambda}{1-\lambda}\int_0^k F\,dx+\left\{\tan\delta_0+\frac{q_0\,C_1}{p_0-p_r}-\frac{C_2}{C_1}\right\}\int_0^k F^2\,dx+\text{constant} \tag{22}$$

$$\left(1+\frac{2\lambda}{k(1-\lambda)}\right)\int_0^k F\,dx+\frac{C_2}{C_1}\int_0^k F^2\,dx = \text{constant}. \tag{23}$$

As in optimisation of H, the calculus of variations shows F to be constant for minimum drag. Hence to the accuracy of the analysis, the optimum inviscid performance of a two-dimensional surface in supersonic flow is given by a 'double wedge' surface (e.g. Fig. 6) with the discontinuity in slope occurring at the point where the pressure change reflected from the shock wave just fails to affect the surface.

With F and H as constants the constant lift condition (equation (12)) becomes

$$kF+(1-k)\,H+\frac{C_2}{C_1}(kF^2+(1-k)\,H^2)+\frac{2\lambda F}{1-\lambda} = 0 \tag{24}$$

i.e.

$$\left(\frac{2\lambda}{1-\lambda}+k\right)F+(1-k)\,H = 0(\delta^2). \tag{25}$$

Then substituting for H^2 in equation (24) from equation (25)

$$H = -F\frac{(k-k\,\lambda+2\lambda)}{(1-k)\,(1-\lambda)}\;1-\frac{C_2\,F(1+\lambda)}{C_1\,(1-k)\,(1-\lambda)}\;+0(F^3). \tag{26}$$

The value of the angle at the discontinuity (Φ) is given by

$$\Phi = H-F. \tag{27}$$

Using equation (26) this becomes

$$\Phi = -\frac{F(1+\lambda)}{(1-k)\,(1-\lambda)}\left(1-\frac{C_2}{C_1}\frac{(k-k\,\lambda+2\lambda)}{(1-k)\,(1-\lambda)}F\right)+0(F^3). \tag{28}$$

From equation (17) the drag is

$$\frac{D-D_0}{(p_0-p_r)\sec^2\delta_0} = -\frac{2\lambda F}{1-\lambda}+\left\{\tan\delta_0+\frac{q_0\,C_1}{p_0-p_r}-\frac{C_2}{C_1}\right\}\left(kF^2+(1-k)H^2\right). \tag{29}$$

Substituting for H^2 from equation (26)

$$\frac{D-D_0}{(p_0-p_r)\sec^2\delta_0} = -\frac{2\lambda F}{1-\lambda}+\frac{BF^2}{(1-\lambda)^2} \tag{30}$$

where

$$B = \frac{k+2\lambda\,k-3\lambda^2\,k+4\lambda^2}{1-k}\left\{\tan\delta_0+\frac{q_0\,C_1}{p_0-p_r}-\frac{C_2}{C_1}\right\}. \tag{31}$$

For the minimum drag $dD/dF = 0$.
i.e.

$$\frac{2\lambda}{1-\lambda} = \frac{2B\,F_{\mathrm{opt}}}{(1-\lambda)^2}. \tag{32}$$

Hence, from equation (28)

$$\Phi_{\mathrm{opt}} = \frac{-\lambda(1+\lambda)}{B(1-k)}\left\{1-\frac{C_2}{C_1}\,\frac{k-k\lambda+2\lambda}{1-k}\cdot\frac{\lambda}{B}\right\} \tag{33}$$

and from equation (30)

$$\frac{D_{\min}-D_0}{(p_0-p_r)\sec^2\delta_0} = -\frac{\lambda^2}{B}. \tag{34}$$

Now $L_0 = p_0 - p_r$ and $L_0/D_0 = \tan\delta_0$, hence equation (34) can be written

$$\frac{D_{\min}-D_0}{D_0} = -\frac{2\lambda^2}{B\sin 2\delta_0}. \tag{35}$$

5. *Further Properties of the Minimum Drag Surface.*

In Section 4 the minimum drag surface was shown to be a double wedge, with a change of surface slope (Φ_{opt}) at the point where the pressure change reflected from the shock wave just fails to affect the surface. The magnitude of Φ_{opt} is of order λ (*see* equation (33)), and its value calculated from equation (33) with $p_r = p_\infty$ and various M_∞ is shown in Fig. 7. As the wedge angle (δ_0) tends to zero, $\Phi_{\mathrm{opt}} \to o$, in accordance with the linear theory result. For $M_\infty = 2$ the value of Φ_{opt} is negative and the optimum surface is slightly convex. For $M_\infty = 3$, it can be seen from Fig. 5 that except close to shock detachment $\lambda \approx o$. Hence the optimum surface at $M_\infty = 3$ is very close to a plane wedge. For Mach numbers greater than $M_\infty = 3$, the optimum surface is concave (except again near shock detachment) and increasing the Mach number with constant wedge angle increases the concavity.

The decrease in drag is shown by equation (35) to be of order λ^2. However, since the optimum shapes are found to avoid the reflected pressure changes impinging on the surface, their performance can be calculated exactly by shock-expansion theory or a double application of oblique shock wave theory. Hence we may determine the accuracy of the present theory by comparing it with exact values. A fairly extreme example is given by $M_\infty = 10, \delta_0 = 20°$ and $\lambda = -0{\cdot}09$. In Fig. 8 the exact value of L/D for the plane wedge and the double wedge (with $\delta_0 = 20°$) is shown with $p_r = p_\infty$. Values from the present theory are shown to be close to the exact values, although as $M\delta$ becomes large some discrepancy occurs.

In Fig. 9 the value of $(D_0 - D_{\min})/D_0$ from equation (35) is shown for various Mach numbers with $p_r = p_\infty$. The decrease in drag compared with the plane wedge with the same lift is very small except at hypersonic Mach numbers or near shock detachment. The accuracy of Fig. 9 is demonstrated by comparing it with the exact configurations shown in Figs. 10 and 11. For the extreme case of Fig. 11 (i.e. $M_\infty = 10$, $\delta_0 = 20°$) Fig. 9 is seen to be in error by 20 per cent. The error is smaller for a lower Mach number or a change in δ_0.

The optimum double wedges described by Figs. 7 and 9, were evaluated using a reference pressure $p_r = p_\infty$. This represents a wedge with a streamwise upper surface and a base pressure equal to free stream static pressure. With little further effort we can consider wedges with base pressures different from free stream static pressure, wedges with fixed upper surfaces, and wedges where the upper surface is the same shape as the lower surface (i.e. thin aerofoils as Fig. 12). The first of these is investigated simply by substituting the base pressure for p_r. If the base pressure is smaller than free stream static pressure the effect is merely to decrease the value of B *via* the term $q_0\, C_1/(p_0-p_r)$ (*see* equation (31)). Hence the optimum shape is a double wedge with a Φ_{opt} of slightly larger magnitude than that which was obtained for $p_r = p_\infty$. There would also be an increase in the value of $(D_{min}-D_0)/D_0$ compared with that shown in Fig. 9. At hypersonic Mach number $p_0 \gg p_\infty$ and changes of base pressure cause little change in B.

The inclusion of a fixed upper surface which does not interfere with the lower surface flow, gives equal lift and drag contributions to the plane and optimum wedges, and so causes no change in the optimisation process of Section 4. Hence the optimum is a double wedge with a Φ_{opt} of the same value as that found for the wedge with upper surface parallel to the free stream.

For expansion surfaces which are perturbed, the pressure change equation equivalent to equation (5) is

$$\frac{p-p_e}{q_e} = C_1\,(M_e)\,\delta_e(x_1)+C_2\,(M_e)\,\delta_e^2(x_1) \tag{36}$$

where subscript e refers to the conditions on the unperturbed expansion surface. As equation (36) contains no term in λ, the optimum surface is a plane. For thin aerofoils, the upper and lower surface values of δ_0 and δ are the same. Hence the lift of a thin aerofoil is given by

$$L = \int_0^1 (p_0-p_e)\,dx+\int_0^1 \left\{q_0\,C_1\,(M_0)-q_eC_1\,(M_e)\right\}\delta(x)\,dx$$

$$+\int_0^1 \left\{(q_0\,C_2\,(M_0)+q_e\,C_2\,(M_e))\,\delta^2(x)+\frac{2\lambda\,C_1\,(M_0)}{1-\lambda}\,\delta(kx)\right\}\,dx \tag{37}$$

and the drag similarly by an expression differing from equation (15) only in the value of its coefficients. The optimisation then proceeds as that of Section 4, resulting in a double wedge optimum whose Φ_{opt} is smaller than that of the equivalent wedge value. It corresponds to a compromise between the larger Φ_{opt} of the compression surface and the zero Φ_{opt} of the expansion surface when they are optimised independently. At hypersonic Mach numbers, when the upper surface pressures are small, the difference between Φ_{opt} for the wedge and the aerofoil is also small.

6. *The Hypersonic Small-Disturbance Theory Result.*

Recently, the optimum two-dimensional surface within hypersonic small-disturbance theory (i.e. $M_\infty \to \infty, \delta_0 \ll 1, M_\infty\,\delta \to \infty$) has been treated by Cole and Aroesty[3]. They do not obtain a strict optimum however and they suggest a 'multi-wedge' as a limited optimum shape.

The analysis of Sections 2 to 4 is only applicable for $M_0\,\delta \ll 1$. As $\delta = 0(\lambda)$ (*see* equations (9) and (32)), this is equivalent to $M_0\,\lambda \ll 1$. When M_∞ is large and δ_0 small the Mach number behind the shock wave (M_0) is large. For $M_\infty \leqq 10$ it can be seen from Fig. 5 that if δ_0 is small then λ is very small and the requirement is still fulfilled.

With δ_0 small (positive) and $M_\infty \to \infty$, it can be seen from Fig. 5 that $\lambda \sim 0{\cdot}14$, and the analysis of Sections 2 to 4 is not applicable. However it is not difficult to adapt this analysis to comply with the hypersonic small disturbance theory assumptions.

The pressure coefficient for the plane wedge is given by hypersonic small disturbance theory to be

$$C_{p0} = (\gamma+1)\,\delta_0^2\,. \tag{38}$$

Then at a wedge angle $\delta_0+\delta$

$$C_p = (\gamma+1)(\delta_0+\delta)^2 \tag{39}$$

$$= C_{p0}+\Delta C_p$$

where

$$\Delta C_p = (\gamma+1)(2\delta\,\delta_0+\delta^2). \tag{40}$$

This values of C_p includes the effect of reflections from the shock wave, correctly in the case of a plane wedge. These reflections originate on the surface at $k^n x$ (Section 2). If $\delta = \delta(x) = \delta(k^n x)$, as for the general perturbed surface, the reflected pressure changes are different from those accounted for in equation (3). The equation is equivalent to equation (3) of Section 2 is

$$C_p = C_{p0}+\Delta C_p+2\sum_{n=1}^{\infty} \lambda^n(\Delta C_p(k^n x)-\Delta C_p) \tag{41}$$

i.e.

$$C_p-C_{p0} = \frac{1-3\lambda}{1-\lambda}\Delta C_p+\frac{2\lambda}{1-\lambda}\Delta C_p(kx)+2\lambda\sum_{n=1}^{\infty} \lambda^n(\Delta C_p(k^n x)-\Delta C_p(kx)) \tag{42}$$

where

$$\Delta C_p = (\gamma+1)(2\delta_0 \,.\, \delta(x)+\delta^2(x)) \tag{43}$$

The constant lift condition is

$$\int (C_p-C_{p0})\,dx = 0\,. \tag{44}$$

Substituting for C_p-C_{p0} from equation (41), and neglecting terms $0(\delta^3, \delta^2\lambda, \delta\lambda^2)$ as in Section 2,

$$2\delta_0(F_1+H_1)+F_2+H_2+\frac{4\lambda\,\delta_0\,F_1}{k(1-3\lambda)} = 0 \tag{45}$$

where F_n and H_n are again defined by equations (11).

The drag coefficient is given by

$$C_D = \int_0^1 C_p \tan(\delta_0+\delta)\,dx\,. \tag{46}$$

Proceeding again as in Section 2

$$\frac{C_D-C_{D0}}{C_{p0}\sec^2\delta_0} = F_1+H_1+\tan\delta_0\,(H_2+F_2)+(\gamma+1)\left(\frac{1-3\lambda}{1-\lambda}\right)\frac{2\delta_0}{C_{p0}}(F_2+H_2)\,. \tag{47}$$

Equations (45) and (47) have the same form as equations (12) and (16) with C_1, C_2, q_0, $(p_0 - p_r)$, k, D and D_0 replaced by $2\delta_0$, 1, $(\gamma+1)(1-3\lambda/1-\lambda)$, C_{p0}, $k(1-3\lambda/1-\lambda)$, C_D and C_{D0} respectively, and the analysis of equations (18) to (35) is applicable to the present case. Hence the optimum shape again approximates closely to a double wedge (showing that the multi-wedge found in Ref. 3 is a more restricted optimum), and the drag coefficient and second wedge angle are given by

$$\frac{C_{D\min} - C_{D0}}{C_{D0}} = -\frac{2\lambda^2}{B \sin 2\delta_0} \tag{48}$$

and

$$\Phi_{\text{opt}} = \frac{-\lambda(1-\lambda^2)}{B(1-\lambda-k(1-3\lambda))} \left\{ 1 - \frac{1-\lambda}{2\delta_0} \cdot \frac{k(1-3\lambda)-2\lambda}{1-\lambda-k(1-3\lambda)} \cdot \frac{\lambda}{B} \right\} \tag{49}$$

where

$$B = \frac{k(1-3\lambda)}{1-\lambda-k(1-3\lambda)} \left\{ 1+2\lambda-3\lambda^2+\frac{4\lambda^2(1-\lambda)}{k(1-3\lambda)} \right\} \times$$

$$\left\{ \tan\delta_0 + \frac{\gamma+1}{C_{p0}} \cdot \frac{1-3\lambda}{1-\lambda} \cdot 2\delta_0 - \frac{1}{2\delta_0} \right\} . \tag{50}$$

Now

$$C_{p0} = C_{D0} \cot \delta_0 = (\gamma+1)\,\delta_0^2 . \tag{51}$$

Hence neglecting terms $0(\delta_0^2)$

$$\frac{C_{D\min}}{C_{D0}} - 1 = -\frac{\lambda^2}{B\delta_0} \tag{52}$$

and

$$\delta_0 B = \frac{k(1-3\lambda)}{1-\lambda-k(1-3\lambda)} \left\{ 1+2\lambda-3\lambda^2+\frac{4\lambda^2(1-\lambda)}{k(1-3\lambda)} \right\} \frac{3-11\lambda}{2(1-\lambda)} . \tag{53}$$

The values of k and λ for hypersonic small disturbance theory are[3]

$$\lambda = -\frac{1-\Gamma}{1+\Gamma} \tag{54}$$

$$k = \frac{2-\Gamma}{2+\Gamma} \tag{55}$$

where

$$\Gamma = \left(\frac{2(\gamma-1)}{\gamma}\right)^{\frac{1}{2}} . \tag{56}$$

For $\gamma = 1{\cdot}4$, $\lambda = -0{\cdot}139$, $k = 0{\cdot}451$ and

$$\Phi_{opt} = 0{\cdot}14\,\delta_0$$

$$\frac{C_{D\min}}{C_{DO}} - 1 = -0{\cdot}0095\,.$$

7. *The Extension to Waveriders Supporting Two-Dimensional Flow Fields.*

A similar analysis to that for the wedge can be applied to waveriders based on two-dimensional flow fields. The unperturbed waveriders are based on the exact flow about a plane wedge. The method is demonstrated here for a waverider of delta planform. The unperturbed shape is a caret wing, as shown in Fig. 13.

The surface perturbations are kept constant along the intersection of the compression surface with rearward facing Mach planes normal to the vertical plane of symmetry such as the one shown by the dotted line in Fig. 13. The flow then remains two-dimensional to first order. With constant planform, the small changes in the shock wave shape cause small changes in the anhedral angle.

Fig. 14 shows a caret wing in side view, AB, EE' and FT' are rearward facing Mach planes along which the surface perturbation (δ) is constant and the direct pressure change is given by $C_1\,\delta + C_2\,\delta^2$. Prescribing $\delta = \delta(x)$ along OT' is sufficient to prescribe δ over the surface. If O' is unit length in the x direction, the plan area of surface with perturbation $\delta(x)$ is $f(x)$ given by

$$f(x) = sx/k' \qquad 0 \leqq x \leqq k' \tag{57}$$

$$= s\frac{1-x}{1-k'} \qquad k' \leqq x \leqq 1 \tag{58}$$

where k' is the x co-ordinate of F, and s if the wing span.

Now AB is a typical perturbation and BC its reflection from the shock wave.

As in the wedge case AA' is equal to $k\ CC'$. Hence $r(x)$ the ratio of the influenced area ($CC'B'B$) to incident area ($AA_1B'B$) is $1/k$ when A is upstream of E, and zero when A is downstream of F. It can be shown that it varies linearly with x for A between E and F.

As for the wedge, reflected pressures are second order and the third order terms are neglected. Hence to this accuracy it may be assumed that reflected pressures act on the unperturbed surface. Then the reflected pressure due to $\delta(x_1)$ is $r\lambda\ C_1\ \delta(x_1)$, and the total change in pressure is

$$p - p_0 = f(x)\{C_1\,\delta(x) + C_2\,\delta^2(x) + r\lambda\,C_1\,\delta(x)\}\,. \tag{59}$$

Using this expression the constant lift condition becomes (by analysis similar to that for the wedge)

$$F_1 + G_1 + H_1 + \frac{C_2}{C_1}(F_2 + G_2 + H_2) + \frac{2\lambda}{k}(F_1 + G_1') = 0 \tag{60}$$

where

$$F_n = \int_0^k F^n f(x)\,dx \tag{61}$$

$$G_n = \int_k^{k'} G^n f(x)\,dx \tag{62}$$

$$G_1' = \int_k^{k'} G \; \frac{k'-x}{k'-k} \; f(x)\,dx \tag{63}$$

$$H_n = \int_{k'}^{1} H^n f(x)\,dx\,. \tag{64}$$

The equation equivalent to equation (16) for the wedge case is

$$\frac{D-D_0}{(p_0-p_r)\sec^2\delta_0} = F_1+G_1+H_1+\tan\delta_0\,(F_2+G_2+H_2)+\frac{q_0\,C_1}{p_0-p_r}(F_2+G_2+H_2). \tag{65}$$

As F_n, G_n and H_n are all proportional to the span S (*via* $f(x)$), from equation (65) the drag coefficient based on planform area is independent of the span. As S becomes large equation (65) does not degenerate to equation (16) (the equivalent wedge equation) because k and k' are independent of S.

Expressing F_n from equations (57) and (61) as

$$F_n = \int_0^{k^2} S\,\frac{F^n(y)\,dy}{k'}$$

where $y = x^2$, F can be shown to be a constant for minimum drag as in the wedge case. Similarly, H can also be shown to be a constant, but the function G for minimum drag is complicated by the G' term in the constant lift constraint. The form of the function G for minimum drag with F and H constant is given by the calculus of variations to be $G = K_1+K_2x$. The value of G varies according to the area influenced by the reflected pressures from the shock wave. As this area is continuous at k and k', the values of G at these values of x are F and H respectively. The value of K_1 and K_2 can thus be determined to give

$$G = H\left(\frac{x-k}{k'-k}\right) + F\left(\frac{k'-x}{k'-k}\right). \tag{66}$$

Hence for the minimum drag H and F are found from equation (60) to be replaced by

$$H-F = \frac{3k'H}{k'^2+k'k+k^2}+0(H^2) \tag{67}$$

and from equation (66)

$$H-G = (H-F)\frac{(k'-x)}{(k'-k)}+0(H^2)\,. \tag{68}$$

Hence equation (65) can be written in terms of H^2 and H^3, similar to the wedge case, and the optimum value of H, G and F (i.e. δ) found to be

$$\delta = F = (1-K)\frac{\lambda}{B}\frac{K_1}{K_2} \qquad \text{for the region } OE_1'EE_2'0 \text{ (Fig. 14) (Fig. 14)} \tag{69}$$

$$\delta = G = \left(1-K\frac{k'-x}{k'-k}\frac{\lambda K_1}{BK_2}\right) \quad \text{for the region } EE_1'T_1'FT_2'E_2'E \text{ (Fig. 14)} \tag{70}$$

$$\delta = H = \frac{\lambda}{B}\frac{K_1}{K_2} \quad \text{for the region } FT_1'T_2'F \text{ (Fig. 14)} \tag{71}$$

where k is as the wedge case (equation (2))

$$B' = \tan\delta_0 + \frac{q_0}{p_0-p_r}\frac{C_1}{C_1} - \frac{C_2}{C_1} \tag{72}$$

$$k' = 1-(\tan\theta-\tan\delta_0)(\beta-\tan\delta_0)\cos^2\theta \tag{73}$$

$$K = \frac{3k'}{k'^2+kk'+k^2}$$

$$K_1 = \frac{k}{k'}(1-k)+\left(\frac{k'}{k}-1\right)\left[1-\frac{2K}{3}-\left(1-\frac{k}{k'}\right)\left(\frac{2}{3}-\frac{K}{2}\right)\right]$$

$$K_2 = \frac{k^2}{k'}(1-K)^2+1-k'+2(k'-k)\left[1-K+\frac{K^2}{3}-\left(1-\frac{k}{k'}\right)\left(\frac{1}{2}-\frac{2K}{3}+\frac{K^2}{4}\right)\right]$$

The drag compared with that of the caret wing of the same lift is given by

$$\frac{D_{\min}}{D_0}-1 = -\frac{2\lambda^2}{B'\sin 2\delta_0}\cdot\frac{K^2{}_1}{K_2}.$$

This is the same as that for the wedge, except for a factor $\frac{K_1^2 B}{K_2 B'} = \frac{K_1^2 k(1+2\lambda)}{K_2(1-k)}$. This has in general a value 0(1). In particular when $M_\infty = 10$, $\delta_0 = 10°$, then $K_1 = -1{\cdot}55$, $K_2 = 1{\cdot}45$ and $\frac{K_1^2 B}{K_2 B'} = 0{\cdot}7$. The value of $\frac{2\lambda^2}{B\sin 2\delta_0}$ from Fig. 9 is 0·0064, giving a possible drag reduction over that of the caret, for these conditions, of 0·45 per cent. The curvature of the shape has the same sign as that of the wedge at the same C_L and M_∞, for it depends on the sign of λ only. A typical concave surface is shown in Fig. 15. Surfaces similar to this have been evaluated in Ref. 6.

8. *Conclusions.*

The two-dimensional compression surface with minimum pressure drag for given lift is a double wedge surface. The discontinuity in slope is at a point such that disturbances from the discontinuity on reflecting from the shock wave just fail to affect the surface. Except when the shock wave is close to detachment the double wedge is convex for $1{\cdot}4 \lesssim M_\infty \lesssim 3$ and concave for other Mach numbers.

When the expansion and compression surfaces have independent shapes and pressures, the magnitude of the compression surface discontinuity for minimum pressure drag is independent of the expansion surface. However, variation in base pressure does change the magnitude of the discontinuity. With a base pressure equal to free stream static pressure the improvement in drag over that of the plane wedge is very small, except at hypersonic Mach numbers when drag reductions over 1 per cent occur. A reduction in base pressure increases this value slightly.

The optimum thin two-dimensional aerofoil is a double flat plate with a single slope discontinuity. The change in slope at the discontinuity is smaller than that required for the optimum wedge.

The analysis is applied also to include hypersonic small-disturbance theory. The optimum surface is again found to be a double wedge with a reduction of drag compared with the plane wedge of about 1 per cent. This result differs from that of Cole and Aroesty[3], which is an optimum under an arbitrary shape constraint.

Optimum 'waveriders' based on two-dimensional flow fields are based on the flow past a surface for which a change in slope occurs over a finite region of the surface. The slopes on either side of this region are similar to those found for the double wedge, and a small reduction in drag at hypersonic speeds compared with the caret wing can be achieved with a surface which is concave chordwise.

LIST OF SYMBOLS

B	Defined by equation (31)
B'	Defined by equation (72)
C_1, C_2	Defined by equation (1)
D	Drag of perturbed surface
D_0	Drag of plane surface
$D_{\min}$	Drag of minimum-drag surface
F	$\delta(x)$ for $0 \leqq x \leqq k$
F_n	Defined by equation (11)
G	$\delta(x)$, $k \leqq x \leqq k'$
G_n	Defined by equation (62)
G'	Defined by equation (63)
H	$\delta(x)$ for $1 \geqq x \geqq k$ (or k' Section 7)
H_n	Defined by equation (11) (or (64) Section 5)
k	$[1-\beta \tan(\theta-\delta_0)]/[1+\beta \tan(\theta-\delta_0)]$
k'	OF/OT in Fig. 14 or equation (73)
K	A constant
L	Lift of perturbed surface
L_0	Lift of plane surface
M_0	Local Mach number close to surface
M_∞	Free stream Mach number
p	Surface pressure
p_0	Unperturbed surface pressure
Δp	Pressure increment
p_r	Reference pressure
q_0	$\frac{1}{2}\gamma p_0 M_0^2$
x	Streamwise co-ordinate
β	$(M_0^2-1)^{\frac{1}{2}}$
γ	Ratio of specific heats of gas
δ	Perturbation angles of surface
δ_0	Inclination of unperturbed surface to free stream direction
θ	Inclination of shock wave to free stream direction
λ	Attenuation factor of disturbances reflected from the shock wave
Φ	Angle at the discontinuity (equation (27))

REFERENCES

No.	*Author*	*Title, etc.*
1	Leipmann .. .. .. Puckett	*Introduction to aerodynamics of a compressible fluid.* Wiley & Sons, 1947, p. 146.
2	Ames Research Staff	Equations, Tables and Charts for compressible flow. NACA Report 1135, 1953.
3	J. D. Cole and J. Aroesty ..	Optimum hypersonic lifting surfaces close to flat plates. *AIAA Jnl.* Vol. 3, No. 8, p. 1520. August 1965.
4	R. S. Bartlett	High lift-drag ratio double wedges of given volume which support two-dimensional supersonic flow fields. RAE TR.66 306, October 1966.
5	G. G. Chernyi	*Introduction to hypersonic flow.* Academic Press 1961, pp. 171–181.
6	L. H. Townend	On lifting bodies which contain two-dimensional supersonic flows. A.R.C. R. & M. 3383. August 1963.

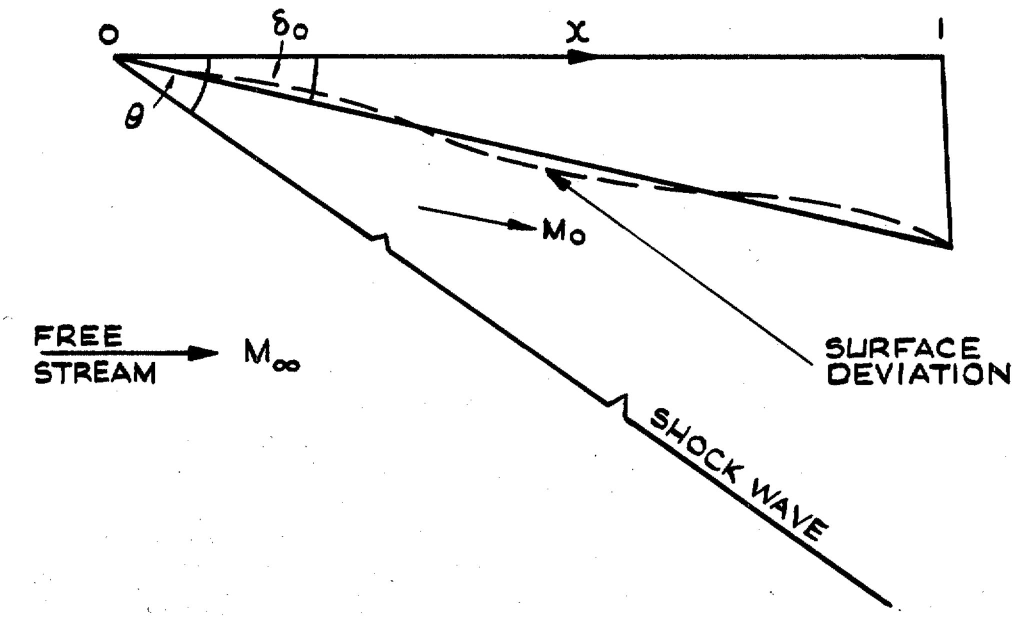

FIG. 1. A plane two-dimensional surface in supersonic flow with small surface deviations (shown dotted).

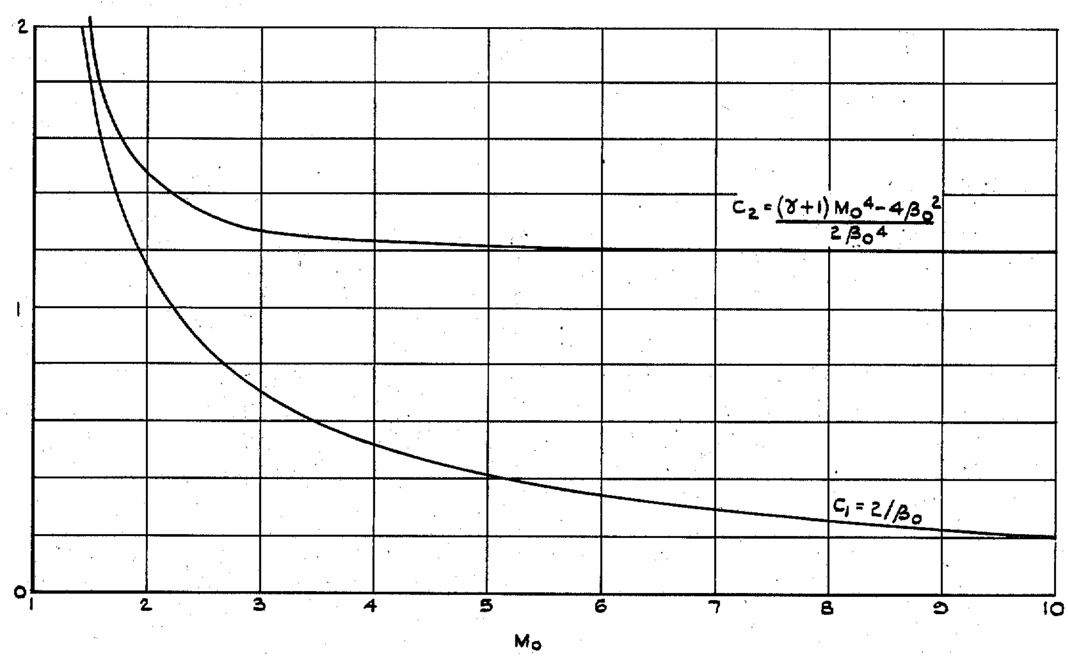

FIG. 2. Values of C_1 and C_2.

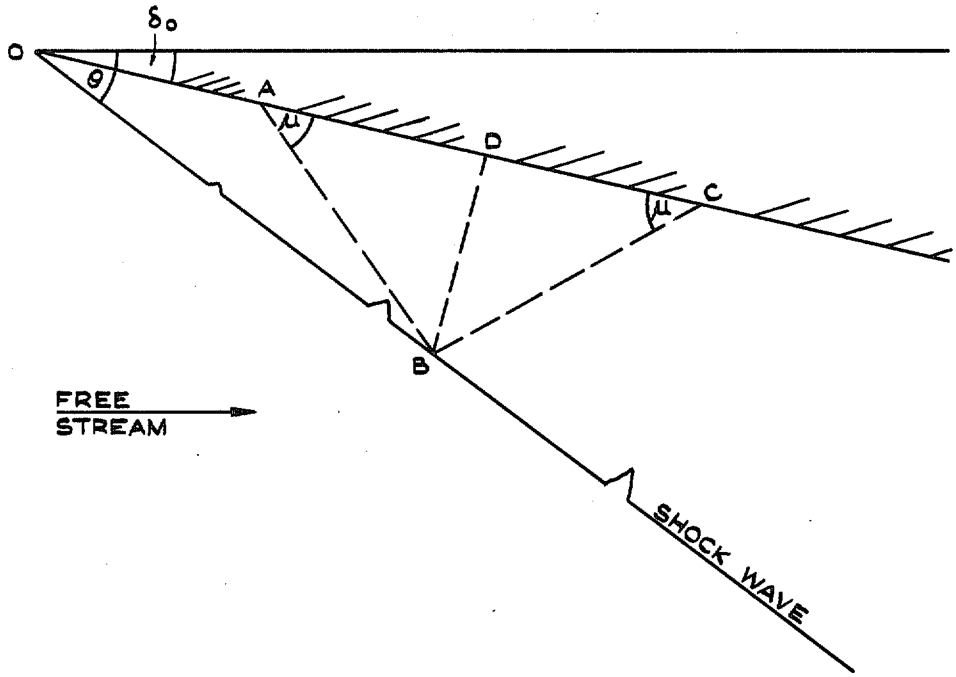

FIG. 3. Reflection path of small disturbances behind a plane shock wave.

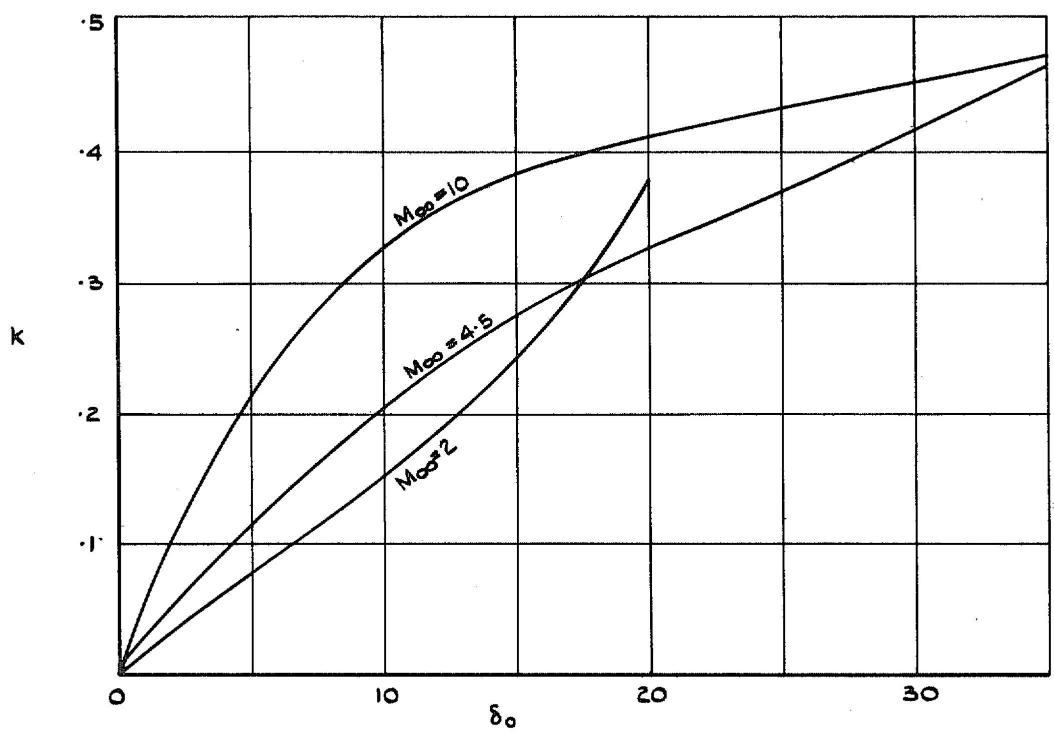

FIG. 4. The value of k.

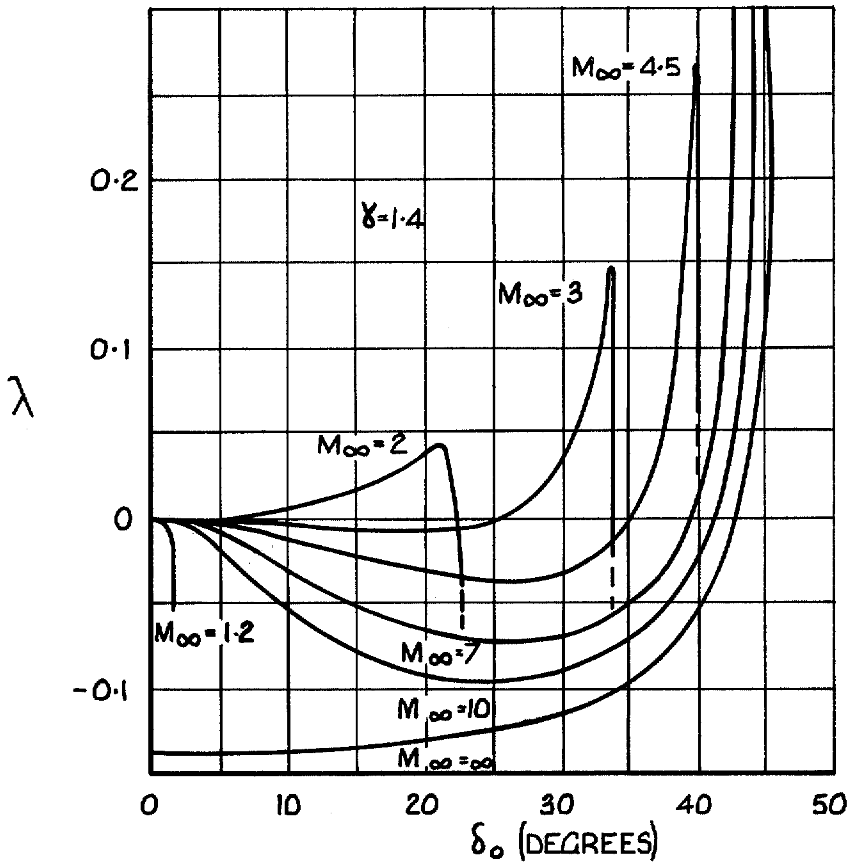

FIG. 5. Reflection coefficient of a disturbance from a shock wave.

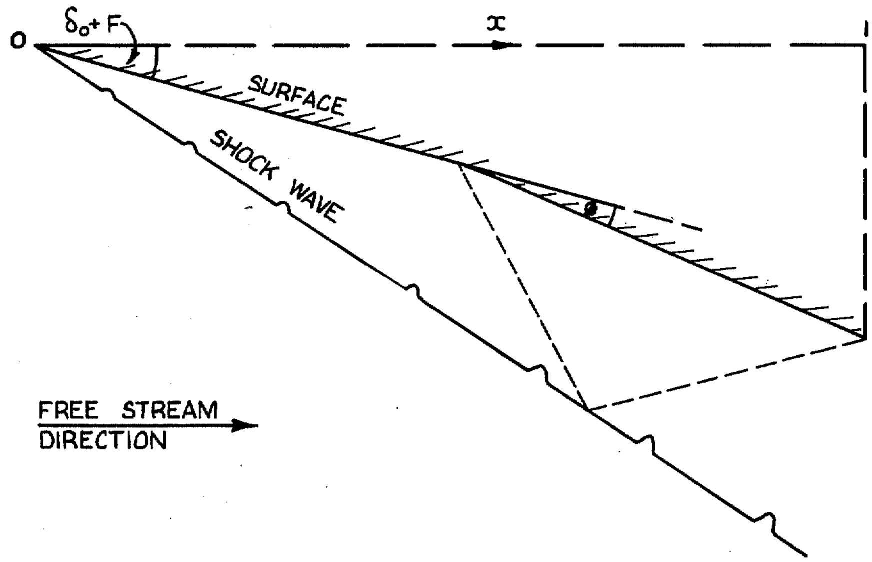

FIG. 6. A 'double wedge' surface.

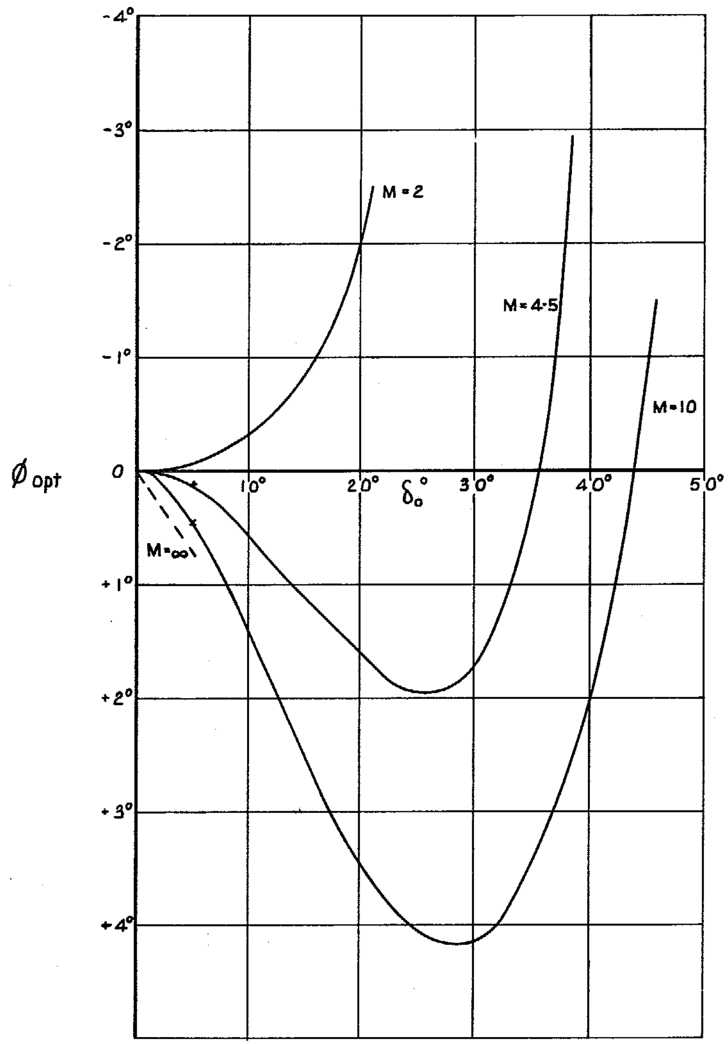

FIG. 7. Optimum second wedge angle for various δ_0 and Mach numbers.

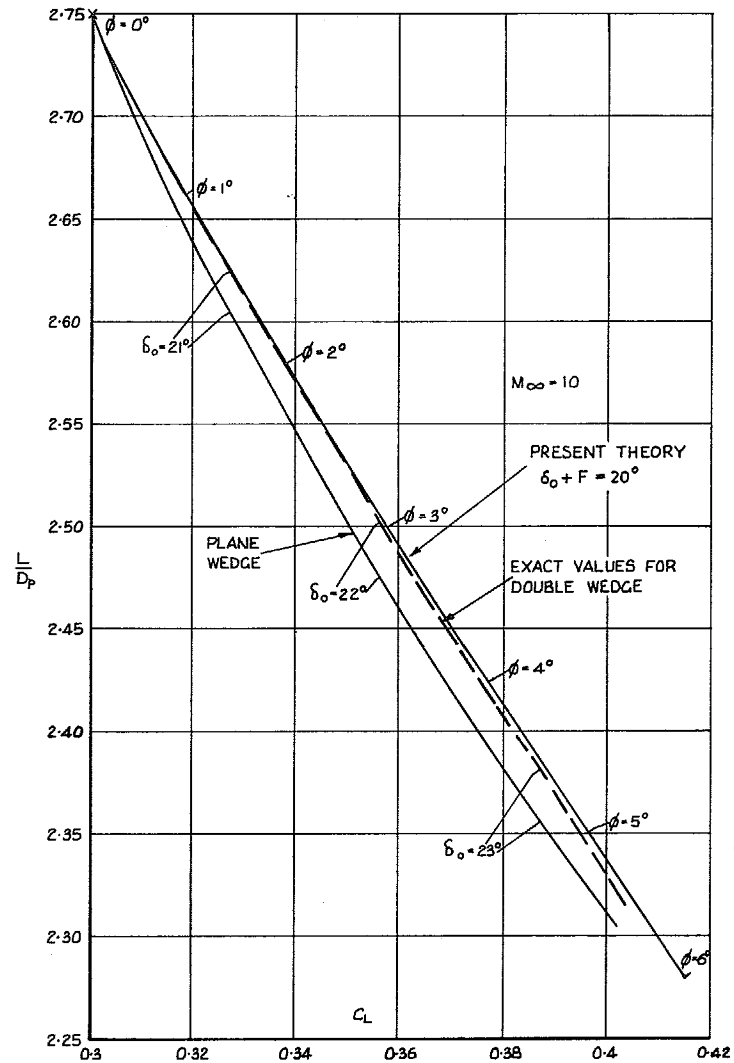

FIG. 8. Comparison of performance of the double wedge with the plane wedge at $M_\infty = 10$, using the present theory and exact values.

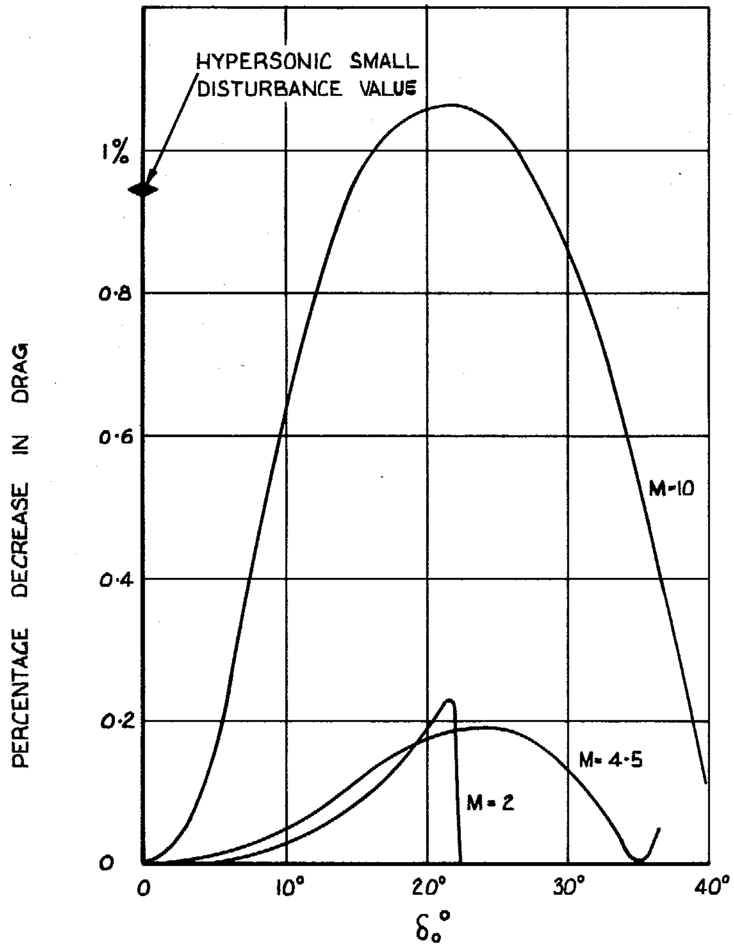

FIG. 9. Percentage reduction in drag of the optimum wedge relative to the plane wedge.

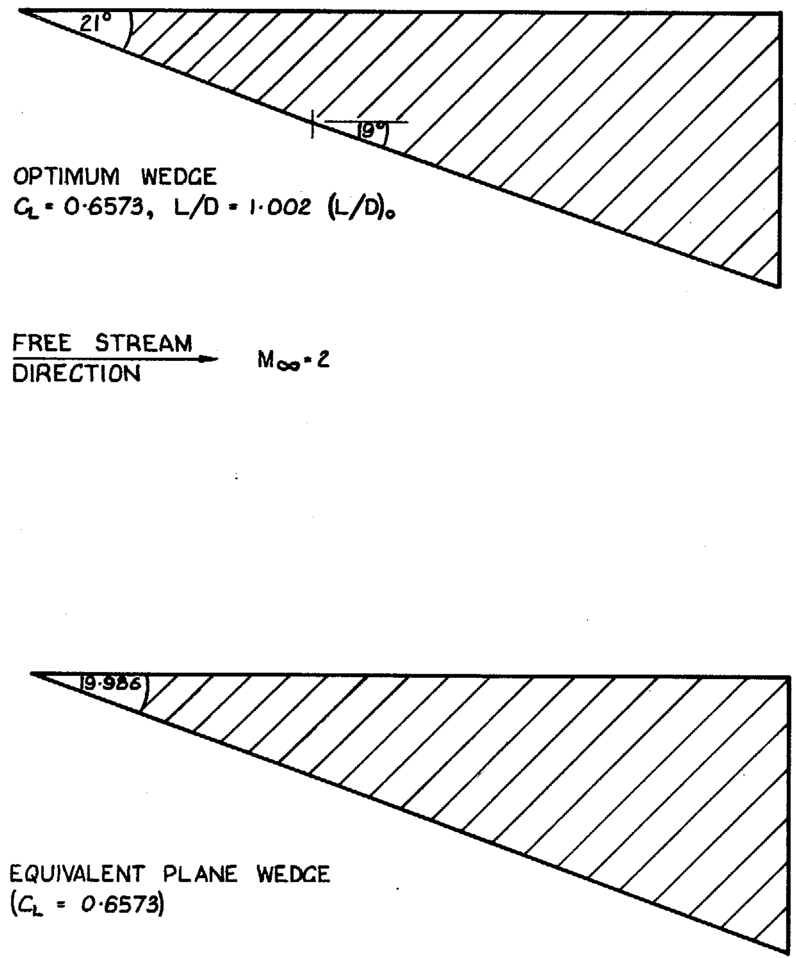

FIG. 10. Optimum wedge and equivalent plane wedge at $M_\infty = 2$.

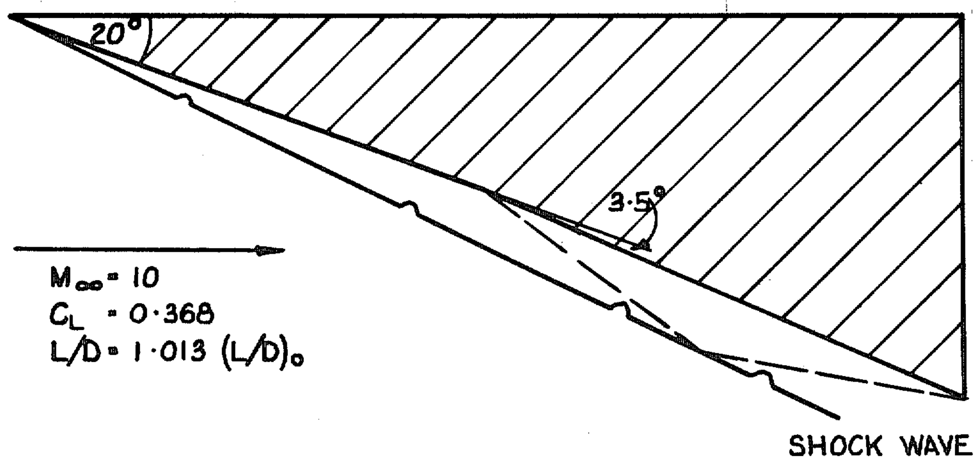

FIG. 11. Optimum lifting wedge at $M_\infty = 10$.

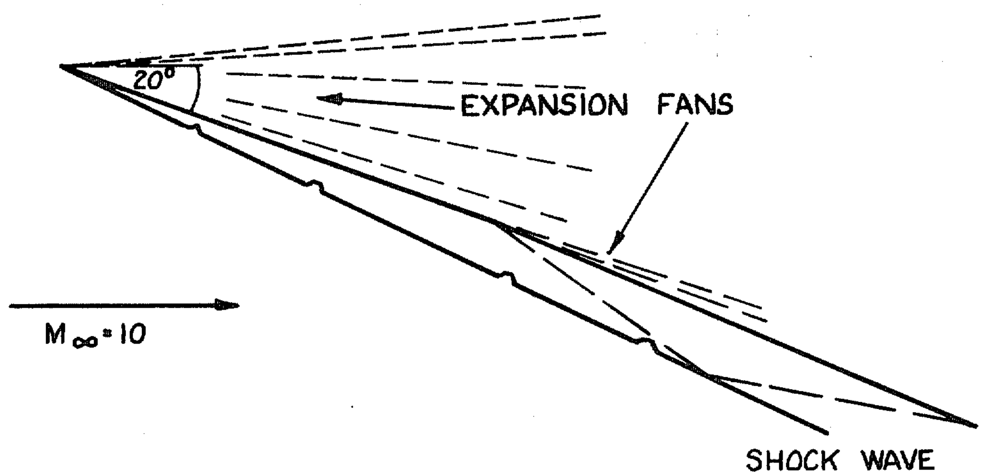

FIG. 12. An optimum two-dimensional aerofoil.

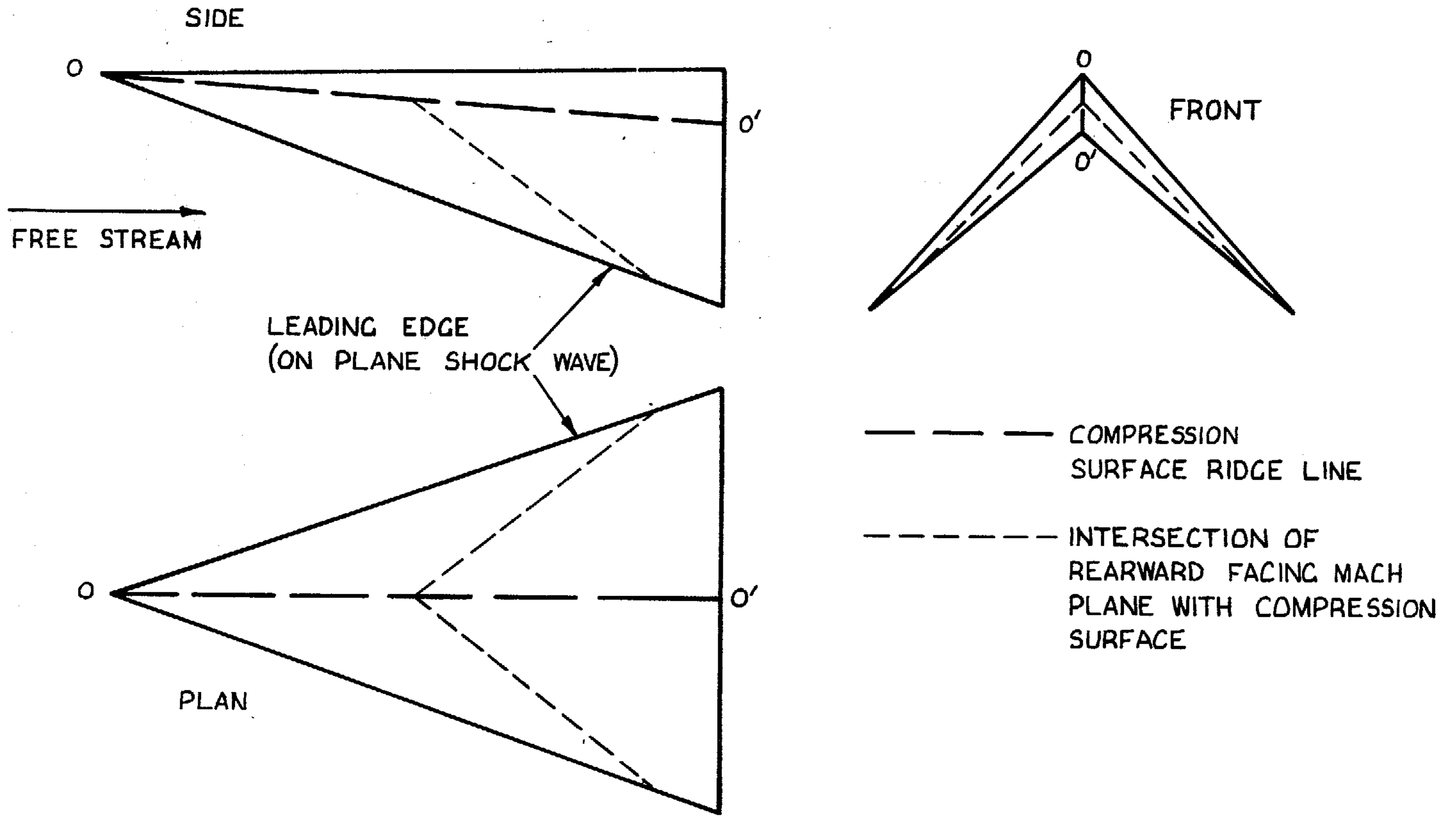

FIG. 13. Caret wing.

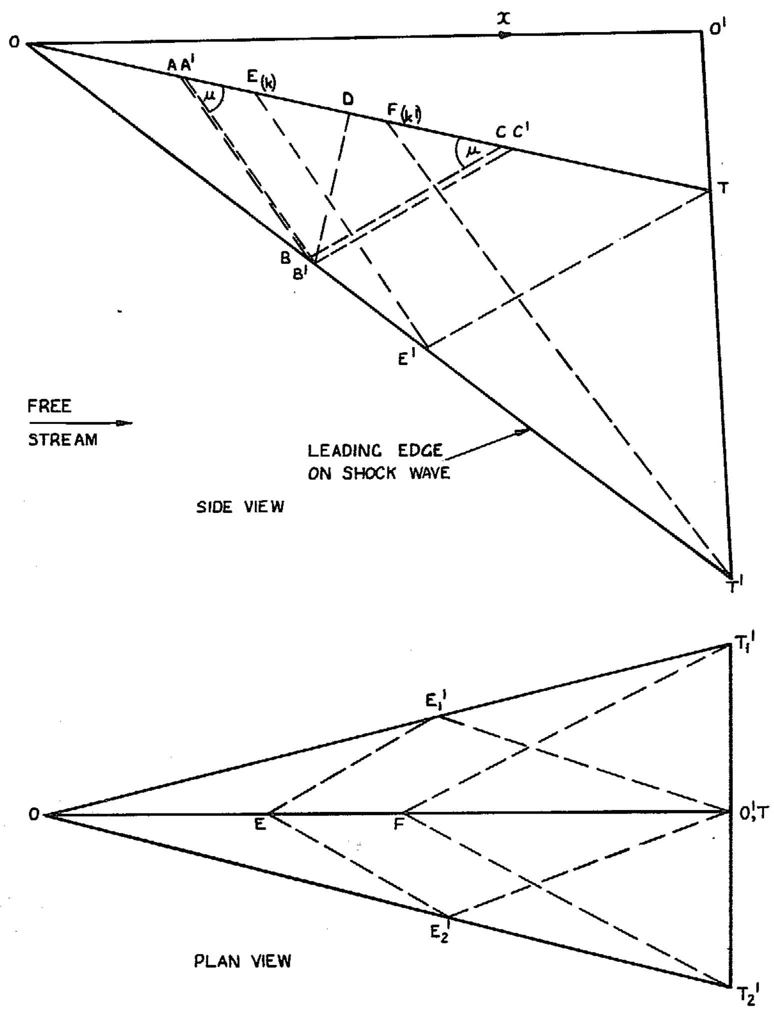

FIG. 14. Caret wing, showing reflected disturbances.

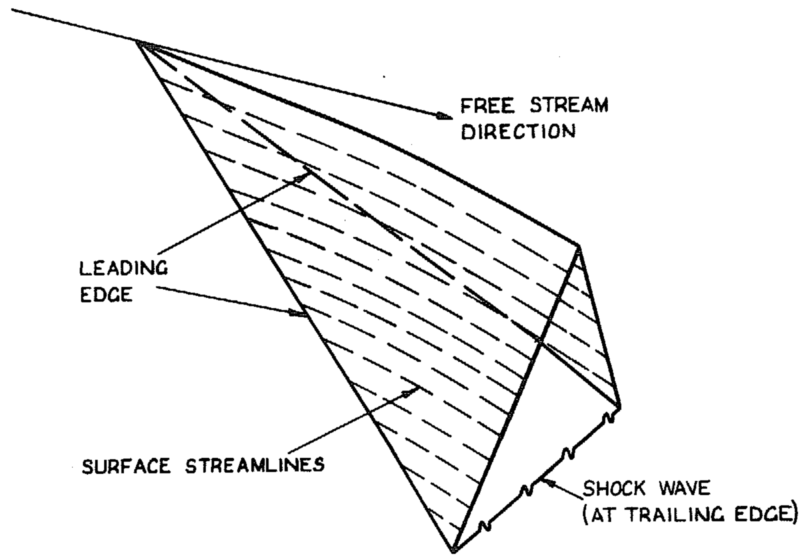

FIG. 15. A typical minimum-drag compression surface based on a two-dimensional flow.

Dd.129527 K.5
Printed in Wales for Her Majesty's Stationery Office by Allens Printers (Wales) Limited

Published by
HER MAJESTY'S STATIONERY OFFICE

To be purchased from
49 High Holborn, London W.C.1
423 Oxford Street, London W.1
13A Castle Street, Edinburgh 2
109 St. Mary Street, Cardiff CF1 1JW
Brazennose Street, Manchester 2
50 Fairfax Street, Bristol 1
258–259 Broad Street, Birmingham 1
7–11 Linenhall Street, Belfast BT2 8AY
or through any bookseller

S.O. Code No. 23-3543